Acta Mech
DOI 10.1007/s00707-010-0392-8

M. de Icaza-Herrera · V. M. Castaño

Generalized Lagrangian of the parametric Foucault pendulum with dissipative forces

Received: 14 April 2008 / Revised: 2 August 2010

Abstract The *Foucault Pendulum* (FP) is a classical mechanical system, particularly interesting because of its sensibility to the rotational motion of Earth, for which has been installed in many scientific laboratories and museums. However, its motion faces two difficulties. The first connected to its decreasing energy, forcing the maintenance staff to restart the movement every day, and the second, that the rotation speed of the plane of oscillation does not match the value predicted by theory. To *understand* the observed motion, the analytical description of the *spherical pendulum*, free of any dissipative process, where the rotation of the Earth along the vertical, depending on the latitude of the observation point is superposed, is utilized in the literature. To truly solve this situation, we propose a Lagrangian that is simultaneously sensitive to the properties of the spherical pendulum and to the rotation of the coordinate system. However, the resulting equations can be solved only under certain limiting conditions, connected to the conservation of certain expressions for energy and for the projection of angular momentum along the vertical. A term corresponding to the *parametric energy feed*, consisting of a change in the length of the wire, in phase with the movement of the pendulum (periodical) was introduced. The new Lagrangian leads to a system of differential equations that can not be solved by analytical methods, and thus, the Runge–Kutta method is employed. To characterize the accuracy of our method, we applied it first to the differential equations that can be solved analytically, in order to see the numerical difference. After demonstrating that such differences are negligible, we focused on determining how accurately are satisfied the assumptions leading to the *analytically solvable problem*, i.e., the constancy of certain expressions for the energy and for the projection of the angular momentum along the vertical, which are shown to be smaller than 35 and 10 parts in a million. Finally, we solve the problem that includes both dissipative forces and parametric energizing. We have installed an actual FP in the *Centro Educativo y Cultural Manuel Gomez Morín del Estado de Querétaro* in Central Mexico, whose motion is made up of a complex cycle, consisting of 57 and 25 oscillations, the last ones under the parametric energy feed, to experimentally support our model.

1 Introduction

Foucault pendulums represented a turning point in classical dynamics as their precession, made apparent as its *orbit* is marked in sand, attest the rotation of the Earth [1]. However, as soon as careful measurements are made, the rate of advance does not fall exactly within the predicted values [2,3]. Moreover, to account for the energy loss that eventually stops the pendulum, several mechanisms have been devised, producing a motion even more complicated.

M. de Icaza-Herrera · V. M. Castaño (✉)
Centro de Física Aplicada y Tecnología Avanzada, Universidad Nacional Autónoma de México,
A.P. 1-1010, Querétaro, Qro 76000, Mexico
E-mail: castano@fata.unam.mx

The physical principle of the *parametric Foucault pendulum* [4] was easily implemented in the pendulum we have designed and constructed in the *Centro Cultural Manuel Gómez Morín*, in the city of Querétaro, in central Mexico, whose length is 28.5 m, its design amplitude, five degrees and the bob's mass, 280 kg. The object of this paper is first to propose a Lagrangian then to choose the right variables to identify the initial conditions. The Lagrangian equations are then integrated using the Runge–Kutta method. From these solutions, we can check the simplifying assumptions and, not only explain the *unexpected* behavior, but to make it clear what should be made to observe the expected motion.

Since the influence of energy loss and of parametric energy feed on the precession of the pendulum is unknown, we establish a Lagrangian that includes parametric excitation, while dissipative forces are taken into account through the so-called Rayleigh function. This approach will provide us with the most general second-order differential equations, having as special case the one corresponding to no dissipative forces and no parametric excitation. These are thus called *general equations* in what follows.

We shall, however, write a second set of differential equations corresponding to an *idealized* Foucault pendulum, without parametric excitation, while dissipative forces and *enough* terms are neglected, so that the solution may be obtained in terms of analytic functions. As known [5], this problem may be stated as a couple of first-order differential equations.

In this paper, these equations are then converted to second order ones, producing thus the *reference equations*, so that our numerical methods will be applied, in all cases, to a couple of second-order differential equations. Our first objective is to compare the numerical with the analytical solution of the reference equations, obtaining thus a graphical idea of how appropriate the first ones result. Having thus got confidence on our numerical methods, we proceed with the following problems:

- The general equations, in the special case of no dissipative forces and no parametric energy feed, are integrated and compared against the numerical solution of the reference equations. Since the reference equations depend on the constancy of the areal velocity and on other assumptions that enable us to neglect several terms in the energy, this comparison is useful and provides a graphical picture of the influence of the neglected terms. The basic idea is to know how well are Foucault pendulums represented by the reference equations. We shall find that the difference between these two methods is negligible.
- Dissipative forces are included, using the general equations, with no parametric feed of energy. We find again that the difference in precession velocity is negligible, while the amplitude and the period decrease.
- Finally, both parametric energy feed and dissipative forces are included and the results compared with those, also obtained from the general equations, but without dissipative forces and without parametric energy feed. We shall find:
  - that the difference in precession velocity is negligible,
  - the influence of both effects on the amplitude and on the period.

2 Reference frames

We shall employ three frames:

K_0 is a reference frame whose Z_0 axis is chosen parallel to the actual axis of rotation of the Earth, its X_0 axis points along the direction of the Spring Equinox, whereas its origin is located at the *apparent-center* A, a point chosen from the Earth's axis of rotation, to be specified below.[1] We shall neglect the precession of the equinoxes, the so-called nutation, and the very small centripetal acceleration of the Earth towards the Sun. Under these assumptions, K_0 is an inertial frame.

K_1 is a reference frame fixed to the Earth, so that
- A is the origin
- Axis Z_1 points from A to the suspension point of the pendulum Q. Let λ' stands for the latitude of Q.
- Axis Y_1, parallel to the West direction[2] at Q, is perpendicular to the plane determined by axis Z_0 and Z_1.
- Axis X_1 is chosen so that $X_1Y_1Z_1$ is an orthogonal right-handed system. Remark that X_1 is *almost* parallel to the direction pointing to the geographical North at Q.

K is a reference frame also fixed to the Earth, whose axes are parallel to those of K_1, but its origin is located at point Q.

[1] See Sect. 2.1.

[2] Tangent to the surface of the Earth.

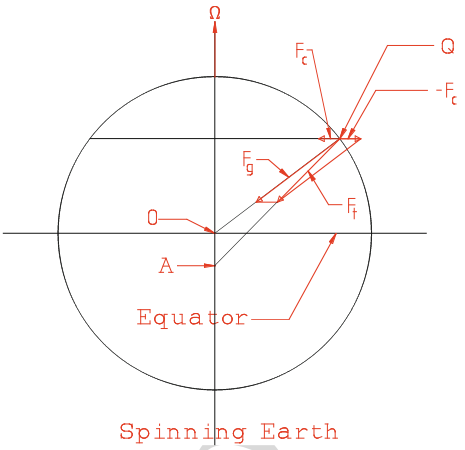

Fig. 1 The vertical axis Z_0 coincides with the rotation axis, Ω is the angular velocity and the apparent-center A of the Earth is that point in the axis of rotation where the resulting sum of gravity, minus centripetal acceleration is directed

2.1 The apparent-center A

Let A be a point in the Earth's rotation axis such that the line from A to the suspension point of the pendulum Q is parallel to the direction of effective gravity. With this choice, the force due to the effective gravity will not exert along this line a non-vanishing torque. This point is the *apparent-center*.

Figure 1 shows a section of the Earth on the Z_0X_0 plane. The Z_0 axis represents the rotation axis, O is the center of the Earth and Q the suspension point of the pendulum. The gravity force is represented by the vector $\mathbf{F}_g = -mg\,\hat{\mathbf{z}}'$, where $\hat{\mathbf{z}}'$ is a unit vector pointing from point O to point Q (radial direction) and g, the acceleration of gravity (in absence of rotation). A particle at Q describes a circle $\mathcal{C}$ perpendicular to the axis of rotation, the so-called *parallel* at the corresponding latitude. To accomplish this, a centripetal force $\mathbf{F}_c = -m\Omega^2(\rho' \cos\lambda')\hat{\imath}$ must be applied to the particle, where $\hat{\imath}$ is a unit vector pointing from the center of $\mathcal{C}$ to Q and ρ' is the radius of the Earth. After applying this force, from the original force $\mathbf{F}_g$, there remains only $\mathbf{F}_t = \mathbf{F}_g + \hat{\imath}\, m\Omega^2\rho' \cos\lambda'$, directed towards the *apparent-center* point A.$\mathbf{F}_t$ is the effective force of gravity. When the point Q is in the plane Z_0X_0, we can write $\hat{\mathbf{z}}'$ as $(\cos\lambda', 0, \sin\lambda')$. To simplify equations, in what follows we shall write $\hat{\mathbf{z}}' = (\kappa', 0, \sigma')$. $\mathbf{F}_t$ is given by

$$\mathbf{F}_t = m\left((\rho'\,\Omega^2 - g)\kappa', 0, -g\sigma'\right) = -m\gamma\,\hat{\mathbf{z}} \tag{1}$$

where $\hat{\mathbf{z}}$, *the vertical*, is antiparallel to the direction given by a standing still pendulum, i.e., a plummet. The effective acceleration of gravity γ is given by

$$\gamma = \sqrt{g^2 - \kappa'^2(2g\rho'\Omega^2 - \rho'^2\Omega^4)} \approx g - \Omega^2\kappa'^2\rho' \tag{2}$$

whereas $\hat{\mathbf{z}}$ is given by

$$\hat{\mathbf{z}} = \frac{((g - \rho'\Omega^2)\kappa', 0, g\sigma')}{\gamma} = (\kappa, 0, \sigma). \tag{3}$$

Thus,

$$\kappa = \cos\lambda = \frac{\left(g - \rho'\Omega^2\right)\kappa'}{\gamma} \tag{4}$$

$$\sigma = \sin\lambda = \frac{g\sigma'}{\gamma}. \tag{5}$$

Let us call ϵ the angle from $\hat{\mathbf{z}}'$ (radial direction) to $\hat{\mathbf{z}}$ (vertical direction), that is, $\epsilon = \lambda - \lambda'$. It follows that

$$\sin\epsilon = \frac{\rho\Omega^2\kappa'\sigma'}{\gamma} \approx \frac{\rho\Omega^2\kappa'\sigma'}{g} \tag{6}$$

$$\cos\epsilon = \frac{g - \rho\Omega^2\kappa'^2}{\gamma} \approx 1. \tag{7}$$

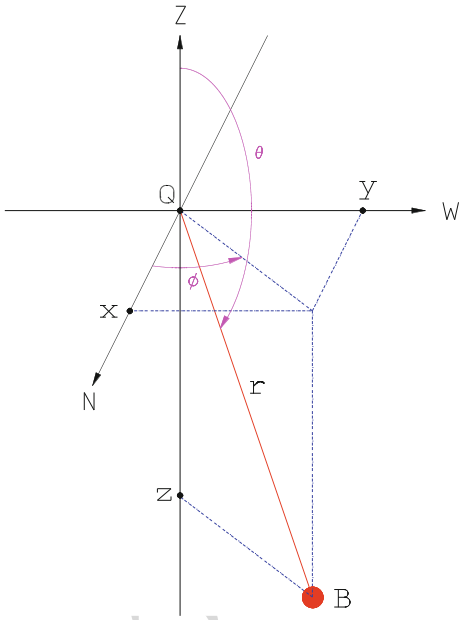

Fig. 2 XYZ coordinates in system K where QZ is the vertical and QY is directed to the West

Also, if we call $\boldsymbol{\rho}$ the vector from point A to point Q, we have

$$\rho\kappa = \rho'\kappa'. \tag{8}$$

Notice that

- ρ, κ and σ are relative to point A, while ρ', κ' and σ', to the center of the Earth
- $\lim_{\Omega\to 0}\epsilon = 0$
- $\sin\epsilon$ goes as Ω^2

In what follows, our equations will be written in terms of κ, σ and ρ, whose expression is greatly simplified by using two constants, depending only on the latitude:

$$\beta_1 = \frac{\gamma\kappa\sigma}{g\left(g-\rho\Omega^2\right)}, \quad \beta_2 = \sqrt{1-\left(\beta_1\rho\Omega^2\right)^2}. \tag{9}$$

2.2 Particle coordinates and the kinetic energy

Let $\mathbf{r}_1$ and $\mathbf{r}$ stand for the position vectors of the bob B, measured in system K_1 and K, respectively, related as

$$\mathbf{r}_1 = \boldsymbol{\rho} + \mathbf{r} \tag{10}$$

where $\boldsymbol{\rho}$, the radius vector from the apparent-center point A to the suspension point Q, is a constant in system K_1 and may be written as $\rho(0, 0, 1)$. $\boldsymbol{\Omega}$ may be written as $\Omega(\kappa, 0, \sigma)$ in both systems K_1 and K_0.

The position $\mathbf{r}$ of the bob B in system K may be described using spherical coordinates: Let $\hat{\mathbf{u}}$ be the unit vector pointing from point Q to the actual position $\mathbf{r}$ of the bob B, as shown in Fig. 2

$$\mathbf{r} = l\hat{\mathbf{u}} = l(\sin\theta\cos\phi, \sin\theta\sin\phi, \cos\theta), \tag{11}$$

where $\theta = \theta(t)$, $\phi = \phi(t)$ and $l = l(t)$ are functions of time t. In the case of a normal pendulum, $l(t)$ is a constant, however, in the case of a parametric pendulum, the value $l(t)$ is imposed by an external mechanism.

The velocity $\mathbf{v}$ is given by:

$$\mathbf{v} = \frac{\mathrm{d}}{\mathrm{d}t}\left[l(t)\hat{\mathbf{u}}\right] = l\left(\dot{\theta}\,\hat{\mathbf{u}}_\theta + \dot{\phi}\,\sin\theta\,\hat{\mathbf{u}}_\phi\right) + \dot{l}\hat{\mathbf{u}}, \tag{12}$$

where $\hat{\mathbf{u}}_\theta$ and $\hat{\mathbf{u}}_\phi$ are given by

$$\hat{\mathbf{u}}_\theta = (\cos\theta\sin\phi, \cos\theta\cos\phi, -\sin\theta) \tag{13}$$

$$\hat{\mathbf{u}}_\phi = (-\sin\phi, \cos\phi, 0). \tag{14}$$

Both systems, K and K_1, measure the same velocity $\mathbf{v}$ for the bob, however, in system K_0, the inertial reference system, the velocity $\mathbf{v}_0$ is given by Coriolis law:

$$\mathbf{v}_0 = \mathbf{v} + \boldsymbol{\Omega} \times (\boldsymbol{\rho} + l\hat{\mathbf{u}}), \tag{15}$$

whose components are:

$$v_{0x} = \cos\phi\left(\dot{l}\sin\theta + l\dot{\theta}\cos\theta\right) - l\sin\theta\sin\phi\left(\sigma\Omega + \dot{\phi}\right) \tag{16}$$

$$v_{0y} = -\kappa\Omega(\rho + l\cos\theta) + \sin\phi\left(\dot{l}\sin\theta + l\dot{\theta}\cos\theta\right) + l\cos\phi\sin\theta\left(\sigma\Omega + \dot{\phi}\right) \tag{17}$$

$$v_{0z} = \dot{l}\cos\theta + l\sin\theta\left(\kappa\Omega\sin\phi - \dot{\theta}\right). \tag{18}$$

The kinetic energy E_k in systems K_1 and K, calculated from $\mathbf{v}$, is given by:

$$E_k = \frac{1}{2}m\left[l^2\left(\dot{\theta}^2 + \dot{\phi}^2\sin^2\theta\right) + \dot{l}^2\right] \tag{19}$$

whereas in system K_0, the kinetic energy E_{k0} using Eqs. 16–18 is given by

$$\begin{aligned} E_{k0} = \frac{m}{2}\Big\{&\left[\dot{l}\cos\theta + l\sin\theta\left(\kappa\Omega\sin\phi - \dot{\theta}\right)\right]^2 \\ &+ \left[-\kappa\Omega(\rho + l\cos\theta) + \sin\phi\left(\dot{l}\sin\theta + l\dot{\theta}\cos\theta\right)\right. \\ &\left. + l\cos\phi\sin\theta\left(\sigma\Omega + \dot{\phi}\right)\right]^2 \\ &+ \left[\cos\phi\left(\dot{l}\sin\theta + l\dot{\theta}\cos\theta\right) - l\sin\theta\sin\phi\left(\sigma\Omega + \dot{\phi}\right)\right]^2\Big\}. \end{aligned} \tag{20}$$

2.3 The potential energy V

If $\mathbf{r}$ is the position vector of the bob, its potential energy is given by $= mg\,\hat{\mathbf{z}}' \cdot \mathbf{r}$, that is

$$V = mg(-\sin\epsilon, 0, \cos\epsilon)\cdot(x, y, z) = mg\left(\beta_2 z - \beta_1\rho\Omega^2 x\right), \tag{21}$$

where $\hat{\mathbf{z}}'$ and $\mathbf{r}$ are measured in system K, and β_1 and β_2 are given by Eq. 9.

3 The Lagrangian

There are two different ways to calculate the Lagrangian. In K_0, an *Inertial Reference System*, the Lagrangian L is given as the kinetic energy minus the potential energy:

$$\begin{aligned} \frac{2L}{m} = &\dot{l}^2 + l^2\left(\dot{\theta}^2 + \dot{\phi}^2\sin^2\theta\right) - 2gl\beta_2\cos\theta \\ &+ \Omega\left\{-2\kappa\sin\phi\left[\rho\dot{l}\sin\theta + l\dot{\theta}(l + \rho\cos\theta)\right]\right. \\ &\left. - 2l\dot{\phi}\sin\theta\left[\kappa\cos\phi(\rho + l\cos\theta) - l\sigma\sin\theta\right]\right\} \\ &+ \Omega^2\left[2l\rho\left(\kappa^2\cos\theta - \sigma\kappa\sin\theta\cos\phi + g\beta_1\sin\theta\cos\phi\right)\right. \\ &+ \kappa^2\rho^2 + l^2\left(\kappa^2\cos^2\theta - 2\kappa\sigma\sin\theta\cos\theta\cos\phi\right. \\ &\left.\left. + \sigma^2\sin^2\theta\cos^2\phi + \sin^2\theta\sin^2\phi\right)\right]. \end{aligned} \tag{22}$$

In K_1, a rotating reference frame, according to Landau [6], the *Lagrangian* is given by

$$L = \frac{1}{2}mv_1^2 + m\mathbf{v}_1 \cdot \Omega \times \mathbf{r}_1 + \frac{1}{2}m(\Omega \times \mathbf{r}_1)^2 - V \tag{23}$$

where m is the bob's mass, $\mathbf{r}_1$ and $\mathbf{v}_1$ (= $\mathbf{v}$) are the position and velocity of the particle *measured in* K_1. Substitution of Eqs. 10 and 12 into Eq. 23 leads to Eq. 22.

It is known that [7]

- the energy H may be calculated from the Lagrangian according to

$$H = \sum_{i-1}^{n} \dot{q}_i \frac{\partial L}{\partial \dot{q}_i} - L \tag{24}$$

where the sum is extended to all the generalized velocities q_i, $i = 1, \ldots, n$.

- This energy H is conserved, that is, is constant, when the Lagrangian does not depend explicitly on time.

In our case, there are only three generalized velocities: $\dot{l}$, $\dot{\theta}$ and $\dot{\phi}$, so that $n = 3$. Substitution of Eq. 22 in Eq. 24 produces:

$$\begin{aligned}\frac{2H}{m} &= \left[\dot{l}^2 + l^2\dot{\theta}^2 + l^2\dot{\phi}^2\sin^2\theta + 2gl\beta_2\cos\theta\right] \\ &+ \Omega^2\left\{-\kappa^2\rho^2 - 2l\rho\left[\sin\theta\cos\phi(g\beta_1 - \kappa\sigma) + \kappa^2\cos\theta\right]\right. \\ &\left. - l^2\left[\kappa^2\cos^2\theta - \kappa\sigma\sin(2\theta)\cos\phi + \sin^2\theta(\sigma^2\cos^2\phi + \sin^2\phi)\right]\right\}.\end{aligned} \tag{25}$$

We can see that there are two main contributions. The first one, enclosed in rectangular brackets, is that part of the energy that is independent of the angular velocity of the Earth. The second one, proportional to the squared angular velocity, is made up from three contributions, respectively, proportional to ρ^2, $l\rho$ and l^2, where l is the length of the pendulum and ρ is the radius of the Earth. The largest one, $-\kappa^2\rho^2$, is a constant and may be neglected (since the energy is defined up to a constant). Also, the contribution of the term in l^2 may be neglected in comparison with that the term going as $l\rho$. This means that the energy can safely be taken to be given by:

$$\begin{aligned}\frac{2H}{m} &= \dot{l}^2 + l^2\dot{\theta}^2 + l^2\dot{\phi}^2\sin^2\theta + 2gl\beta_2\cos\theta \\ &- 2\Omega^2 l\rho\left[\sin\theta\cos\phi(g\beta_1 - \kappa\sigma) + \kappa^2\cos\theta\right].\end{aligned} \tag{26}$$

3.1 Energy dissipation

There are dissipative forces acting on the pendulum, due to the surrounding air and to the cable. The viscosity force acting on a particle moving in air is given by

$$\mathbf{F} = -k\mathbf{v} \tag{27}$$

where k is a constant depending on both the viscosity of the air and the *form* of the particle. When the particle is a sphere, k is given by the law of Stokes: $k = 6\pi\eta r$, where η is the viscosity, and r is the radius of the sphere.

The bob of our pendulum has a mass of 280 kg while the cable is made up of many thin stainless steel threads. It is the relative motion between these threads, which absorbs a considerable amount of energy. We shall assume that these frictional forces, opposing the deformation of the cable, are also proportional to the velocity of the bob, that is, that they are given by a Eq. 27, with a different value of k, to be determined from experiment. The sum of two such terms may also be written as Eq. 27, where the k now corresponds to the sum of both effects.

According to Goldstein [8], they may be taken into account by means of the so-called *Rayleigh dissipation function*:

$$R(v_x, v_y, v_z) = \frac{1}{2}\left(k_x v_x^2 + k_y v_y^2 + k_z v_z^2\right), \tag{28}$$

where the constant vector (k_x, k_y, k_z) allows the dissipative force to depend on the direction. In our case, we shall write, according to the components of $\mathbf{v}$,

$$R(\theta, \phi, \dot{\theta}, \dot{\phi}) = \frac{ml^2}{2}\left(k_\theta \dot{\theta}^2 + k_\phi \dot{\phi}^2 \sin^2\theta\right), \tag{29}$$

where we have introduced the mass m so that the ensuing equations are simplified. k_θ and k_ϕ have no units.

4 The *general* equations

In these conditions, the equations of motion are [8]:

$$\frac{\mathrm{d}}{\mathrm{d}t}\left(\frac{\partial L}{\partial \dot{\theta}}\right) - \frac{\partial L}{\partial \theta} + \frac{\partial R}{\partial \dot{\theta}} = 0 \tag{30}$$

$$\frac{\mathrm{d}}{\mathrm{d}t}\left(\frac{\partial L}{\partial \dot{\phi}}\right) - \frac{\partial L}{\partial \phi} + \frac{\partial R}{\partial \dot{\phi}} = 0. \tag{31}$$

We obtain respectively:

$$\begin{aligned} &l\ddot{\theta}(t) + \dot{\theta}(k_\theta + 2\dot{l}) - \sin\theta\left(l\dot{\phi}^2\cos\theta + g\beta_2\right) \\ &- 2\Omega\left[l\dot{\phi}\sin\theta\cos\phi(\kappa\sin\theta + \sigma) + \kappa\dot{l}\sin\phi\right] \\ &+ \Omega^2\left\{\rho\cos\theta\cos\phi\left[\kappa^2\sin\theta - 4(g\beta_1 - \kappa\sigma)\right]\right. \\ &\left. + l\left[\kappa\sigma\cos\phi(1 - 2\sin^2\theta) + \sin\theta\cos\theta\left(\kappa^2\cos^2\phi - \sigma^2\right)\right]\right\} = 0 \end{aligned} \tag{32}$$

and

$$\begin{aligned} &-2\dot{\phi}(\dot{l}\sin\theta + l\dot{\theta}\cos\theta) - l\sin\theta\left(k_\phi\dot{\phi} + \ddot{\phi}(t)\right) \\ &+ 2\Omega\left[\dot{l}(\kappa\cos\theta\cos\phi - \sigma\sin\theta) - l\dot{\theta}(\sigma\cos\theta + \kappa\cos\phi\sin\theta)\right] \\ &\Omega^2\sin\phi\left[\rho(\kappa\sigma - g\beta_1) + l\kappa(\sigma\cos\theta + \kappa\cos\phi\sin\theta)\right] = 0. \end{aligned} \tag{33}$$

Equations 32 and 33 describe the motion of a *spherical pendulum* in a rotating reference frame subjected both to parametric excitation and dissipative forces.

The equations of motion for a *normal Foucault pendulum* are obtained from these imposing the constant length, so that $\dot{l} = 0$, and without dissipative forces, that is, $k_\theta = k_\phi = 0$.

5 The *reference* equations

The full analytical treatment [5], however, depends on substituting the two second-order by first-order differential equations. One is obtained from Eq. 26, after neglecting the term in Ω^2:

$$E = \frac{m}{2}\left[l^2\left(\dot{\theta}^2 + \dot{\phi}^2\sin^2\theta\right) + 2l\gamma\cos\theta\right]. \tag{34}$$

While the other from the constancy of the *areal-velocity*, a concept borrowed from *celestial mechanics*. Kepler (1571–1630) established in his second law that:

> A line joining a planet and the sun sweeps out equal areas during equal intervals of time.

This fact, connected with the conservation of *angular momentum*, is shown to hold in the case of the so-called central forces, because the corresponding torques vanish. In our case, we must follow the motion of the bob from the vertical: At time t, the length of the pendulum is l, while the distance from the bob to the vertical is $l\sin\theta$, its angular velocity around the vertical is $\sigma\Omega + \dot{\phi}$, so that its velocity around the vertical is given by $l\sin\theta(\sigma\Omega + \dot{\phi})$. The areal-velocity φ is thus given by

$$\varphi = l^2\sin^2\theta\left(\sigma\Omega + \dot{\phi}\right)/2, \tag{35}$$

whose time rate of change may be calculated with the help of Eq. 33:

$$\frac{\mathrm{d}\,\varphi}{\mathrm{d}\,t} = \frac{\kappa\,\Omega\,\sin\theta}{2}\left\{ -2\dot{\theta}\,\sin\theta\,\cos\phi \right.$$
$$\left. +\,\Omega\,\sin\phi\left[\frac{\rho\sigma}{l}\left(1-\frac{g}{\gamma}\right)+(\sigma\,\cos\theta+\kappa\,\cos\phi\,\sin\theta)\right]\right\}. \tag{36}$$

If the RHS of Eq. 36 is neglected, the areal-velocity $\varphi(t)$ is a constant, φ_0, given by

$$\varphi_0 = l^2\,\sin^2\theta\,\left(\sigma\,\Omega+\dot{\phi}\right)/2 \tag{37}$$

and the resulting equations may be solved in terms of analytic functions.

Equations 34 and 37, first-order differential equations, produce the *standard motion* of the Foucault's pendulum, whose analytical solutions will be given below. However, we are interested in obtaining second-order differential equations from them, to have a simple test of the precision of our numerical solutions: the difference between the numerical and the analytical solutions.

One of these equations $\ddot{\phi}$ is obtained simply taking the time derivative of Eq. 37:

$$\ddot{\phi} = -\frac{2\sqrt{2}\omega_*\sqrt{1-\zeta^2}\sqrt{1-\tau^2}}{\sqrt{\zeta+\tau}}\dot{\theta}\,\csc^2\theta\,\cot\theta \tag{38}$$

where τ, ζ and ω_* are connected with the initial conditions as shown later.

Next, we obtain $\dot{\phi}$ from Eq. 37 and substitute it into Eq. 34. From the resulting equation and its time derivative, we obtain $\ddot{\theta}$:

$$\ddot{\theta} = \frac{\omega_*^2}{\zeta+\tau}\,\csc^3\theta\left[(\zeta+\tau)\,\sin^4\theta+2\left(1-\zeta^2\right)\left(1-\tau^2\right)\cos\theta\right] \tag{39}$$

Equations 38 and 39 are the *reference equations*.

6 Initial conditions

Routinely, however, the time evolution of the system is obtained from the so-called *initial conditions*, that is, the coordinates and velocities at time $t = 0$. In our case, we could use

$$\begin{aligned} \theta(0) &= \theta_0, \quad \dot{\theta}(0) = \dot{\theta}_0 = 0 \\ \phi(0) &= \phi_0, \quad \dot{\phi}(0) = \dot{\phi}_0. \end{aligned} \tag{40}$$

Let T stands for the period of the pendulum. If at time $t = 0$, the pendulum is at its largest deviation from the vertical, at time $t = T/4$, the pendulum will be at its closest approach to the vertical. Instead of conditions at time $t = 0$, Eq. 40, we could use conditions at time $t = T/4$:

$$\begin{aligned} \theta(T/4) &= \theta_1, \quad \dot{\theta}(T/4) = \dot{\theta}_1 = 0 \\ \phi(T/4) &= \phi_1, \quad \dot{\phi}(T/4) = \dot{\phi}_1, \end{aligned} \tag{41}$$

where $\phi_1 - \phi_0$ is the azimuth advance corresponding to $T/4$.

The comparison between theoretical and experimental results involves two different experimental techniques: either the delicate *measurement* of $\dot{\phi}$ or the *preparation* of the pendulum in a physical state corresponding to the initial value given by $\dot{\phi}$.

Since we are interested in a Foucault-type motion, the numerical values of $\dot{\phi}_0$ should be of the same order of magnitude as those of Ω: Typical values of $\dot{\phi}(0)$ are very small. Since the motion of the pendulum may be simply described as a precessing ellipse, we are interested in using conditions connected with its corresponding semi-major and semi-minor axes.

Instead of describing the mechanical motion as a function of the initial values, Eqs. 40 or 41, we would rather use *mixed* information:[3] the θ values at times $t = 0$ and $t = T/4$ [5], which play the rôle of semi-axes of

[3] *Boundary conditions* is the name given to this problem in the frame of the theory of differential equations.

the previously mentioned ellipse. Since these *mixed* conditions may be reduced to the initial conditions given by Eq. 40 for a suitable value of $\dot{\phi}_0$, to be determined from the conservation Eqs. 34 and 37, the problems solved here belong to the class of *initial conditions*. This procedure is straightforward except for the sign: for given values of θ_0 and θ_1, the ellipse may be described counter (positive) or clock-clockwise (negative).

Concerning the numerical values for our initial conditions, we choose for $\pi - \theta(0)$ an arc of five degrees and for $\pi - \theta(T/4)$ an arc of 0.46 min. Concerning this last value, an arc of 4.6 min produces an ellipse precession as large as the *Foucault effect* [5], that is, if the ellipse is described counterclockwise, the rotation velocity vanishes, so that the plane of oscillation seems to be fixed.

$$\theta(0) = \theta_0 = \pi - \frac{\pi}{36} \tag{42}$$

$$\theta(T/4) = \theta_1 = \pi - \frac{23\pi}{540000}. \tag{43}$$

We have defined $\tau = \cos\theta_0$, $\zeta = \cos\theta_1$ and ω_* so that $2\omega_*^2 = 2\omega^2 + \sigma^2\Omega^2(\tau + \zeta)$.

Five different solutions will be presented, so that the different influences may by accurately quantified. Notice that the reference Eqs. 38 and 39 assume no dissipative forces and no parametric energy feed.

- **a** Analytical solutions $\theta_a(t)$ and $\phi_b(t)$ to the reference Eqs. 38 and 39.
- **n** Numerical solutions $\theta_n(t)$ and $\phi_n(t)$ to the reference Eqs. 38 and 39.
- **b** Numerical solutions $\theta_b(t)$ and $\phi_b(t)$ to the general Eqs. 32 and 33 without dissipative forces and without parametric energy feed.
- **c** Numerical solutions $\theta_c(t)$ and $\phi_c(t)$ to the general Eqs. 32 and 33 with dissipative forces but without parametric energy feed.
- **d** Numerical solutions $\theta_d(t)$ and $\phi_d(t)$ to the general Eqs. 32 and 33 with dissipative forces and with parametric energy feed.

7 Analytical solution

Let $\theta_a(t)$ and $\phi_a(t)$ stand for the analytical solution to the reference equations. According to [5], they may be obtained from:

$$t = \sqrt{\frac{2}{\zeta - \tau}}\,\frac{\mathrm{F}(\chi(u)|m)}{\omega_*} \tag{44}$$

$$\phi(u) = -\sigma\Omega\sqrt{\frac{2}{\zeta - \tau}}\,\frac{\mathrm{F}(\chi(u)|m)}{\omega_*} + \sqrt{\frac{(1-\zeta^2)(1-\tau^2)}{(\zeta+\tau)(\zeta-\tau)}}(\delta+\tau) \times \left[\frac{\Pi(n_1;\chi(u)|m)}{(\delta+1)(1-\tau)} + \frac{\Pi(n_2;\chi(u)|m)}{(\delta-1)(1+\tau)} - \frac{2\mathrm{F}(\chi(u)|m)}{(\delta^2-1)(\delta+\tau)}\right] \tag{45}$$

where:

- F and Π are the elliptic functions of first and third kinds [9]:

$$F(x|m) = \int_0^{\sin x} \frac{\mathrm{d}t}{\sqrt{(1-t^2)(1-mt^2)}}$$

$$\Pi(n;x|m) = \int_0^{\sin x} \frac{\mathrm{d}t}{(1-nt^2)\sqrt{(1-t^2)(1-mt^2)}}$$

- The parameters m, n_1, n_2 are given by:

$$m = \frac{\zeta+\delta}{\zeta-\tau}, \quad n_1 = \frac{1+\delta}{1-\tau}, \quad n_2 = \frac{1-\delta}{1+\tau} \tag{46}$$

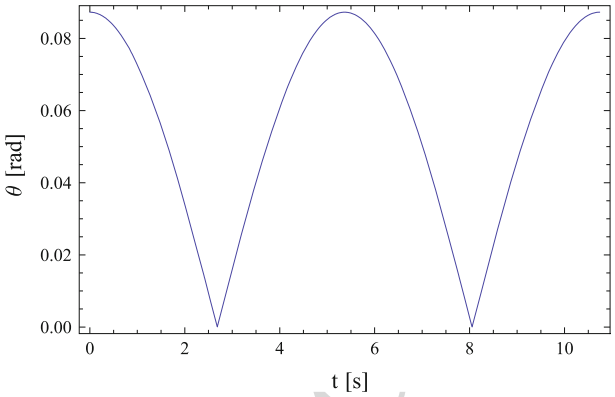

Fig. 3 $\theta(t)$, the angular excursion from the downward vertical, along a full period. This figure, within the graphical precision, represents both the analytical and the numerical solutions. The plot does not touch the time axis since its minimum value is $\theta = 0.00013$ rad. This means that the bob does not go through the vertical. (Notice that the line $\theta = 0$ is not the same as for the lower frame line)

- θ, u and $\chi(u)$ are connected by

$$\chi(u) = \arcsin\left(\sqrt{\frac{u-\tau}{u+\delta}}\right), \quad u = -\cos\theta. \tag{47}$$

The idea is to substitute Eq. 47 into Eq. 44 and then solve for θ, obtaining thus $\theta_a(t)$, while $\phi_a(t) = \phi(-\cos\theta_a(t))$ is obtained in a similar way. Up to this point, θ is measured from the upward direction of the vertical, but in the sequel, we will measure it from the downward direction of the vertical, so that a standing still plummet has $\theta = 0$.

8 Analytical vs. numerical solutions of the *reference* equations

Let T stands for the period of the pendulum. Its numerical value depends on the initial conditions, Eq. 40, which are determined from the *boundary* conditions, Eqs. 42–43, and on whether or not there are dissipative forces and/or energy feed. Since the boundary conditions are fixed, the value of T is close to 10.7 s. In these conditions, at times $t = T/4$ and $t = 3T/4$, the bob is at its closest approach to the vertical, while at $t = 0$ and $t = T/2$, the bob is at the largest excursion from the vertical. The approximate numerical values of these four times are: 0, 2.684, 5.368 and 8.052 s.

Figure 3 shows the angular excursion from the vertical $\theta(t)$ along a full period $[0, T]$.

The plot of $\phi(t)$ behaves as a Heaveside function when the bob approaches the vertical, that is, $\phi(t)$ is essentially a constant function, except when the bob is very close to the vertical, undergoing a very fast change, close to π. For this reason, Fig. 4 shows the azimuth $\phi(t)$ for times close to $t = T/4 = 2.684$, when the bob is close to the vertical.

The analytical functions $\theta_a(t)$ and $\phi_a(t)$ are so close to the numerical solutions $\theta_n(t)$ and $\phi_n(t)$, that Figs. 3 and 4 represent, each one, both solutions. The only way to appreciate the error of the numerical solution is to plot the differences $\theta_n(t) - \theta_a(t)$ and $\phi_n(t) - \phi_a(t)$, as shown in Figs. 5 and 6. Since all these differences are smaller than 3×10^{-19}, we can trust our numerical methods.

9 Accuracy of the *reference* equations

Up to this point, we have compared the analytical to the numerical solutions of the *reference* equations. Now, we would like to compare the motion predicted by the *reference* equations, depending on the conservation (approximate) equations, Eqs. 38–39, against the motion predicted by the *general* equations in the special case of no dissipative forces and no parametric energy feed, that is, setting $k_\theta = k_\phi = 0$ and $\dot{l} = 0$ in Eqs. 32 and 33. This comparison is useful, since it is a test on the validity of the approximations leading to Eqs. 38 and 39.

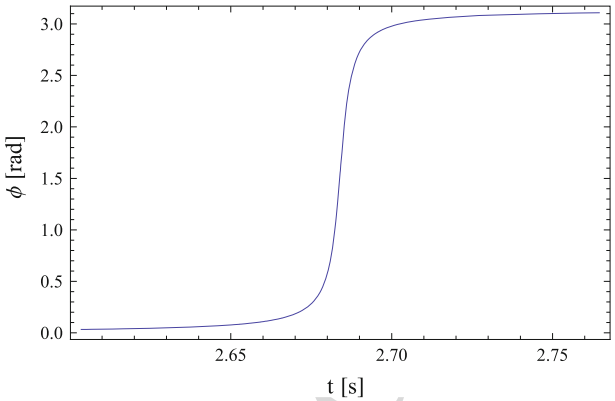

Fig. 4 The azimuth $\phi(t)$ as the bob approaches and then recedes from the vertical. This plot is limited to a small interval around the time of maximum approach to the vertical which occurs at $t = T/4 = 2.68402$

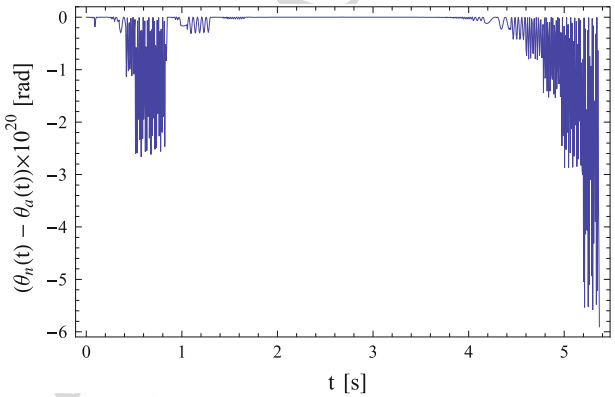

Fig. 5 Difference $\theta_n(t) - \theta_a(t)$ between the numerical and analytical solutions for $\theta(t)$

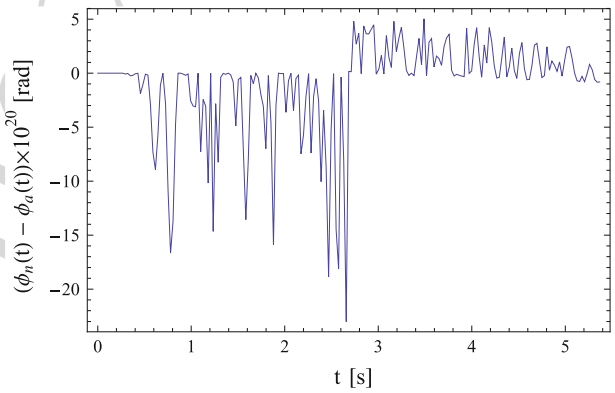

Fig. 6 Difference $\phi_n(t) - \phi_a(t)$ between the analytical and numerical solutions for $\phi(t)$

We shall label $\theta_b(t)$ and $\phi_b(t)$ the corresponding numerical solutions to the thus *restricted general* equations, which are to be compared to the previous ones, i.e., the numerical solution to the reference equations.

A plot of $\theta_b(t)$ can not be distinguished from a plot of $\theta_n(t)$ along a full period, the same being true of a plot of $\phi_b(t)$ when compared with a plot of $\phi_n(t)$. These plots seem to show that both motions are identical; however, a better resolution is obtained by plotting the corresponding differences $\theta_b(t) - \theta_n(t)$ and $\phi_b(t) - \phi_n(t)$, shown in Figs. 7 and 8. The difference $\theta_b(t) - \theta_n(t)$, as shown in Fig. 7, remains below 1 μRad. Although the figure seems to show a discontinuity as the bob approaches the vertical, the behavior is continuous. We should possibly add, concerning Foucault pendulums, that the motion in $\theta(t)$ is not usually considered since it does not exhibit in a simple way the influence of the rotation of the Earth. The motion

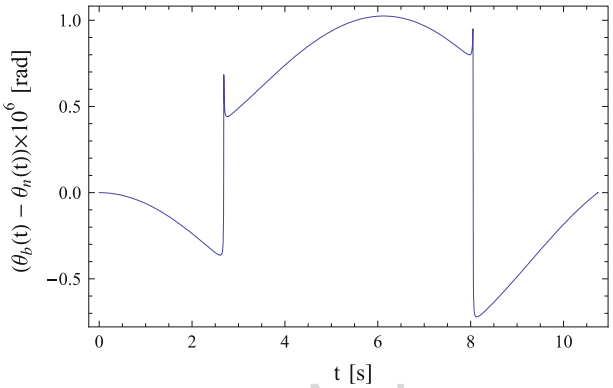

Fig. 7 Difference $\theta_b(t) - \theta_n(t)$ between the numerical solutions to the general and reference equations, respectively. The two apparent discontinuities around $t = T/4$ and $t = 3T/4$ are continuous

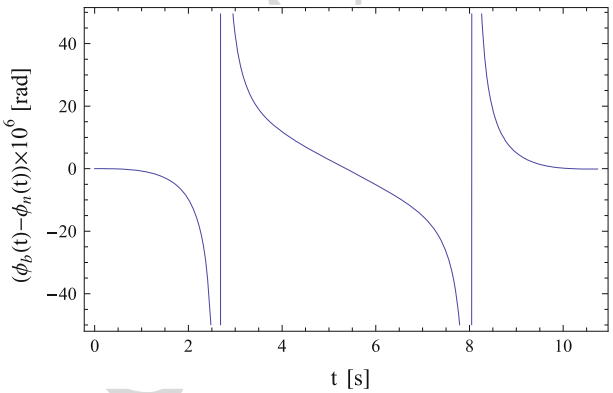

Fig. 8 $\phi_b(t) - \phi_n(t)$, the difference between the solutions to the general equations (no dissipative forces and no parametric energy feed) and to the reference equations

in $\phi(t)$, on the contrary, is carefully recorded *only at the maximum excursions of the bob from the vertical*, and at these times, according to Fig. 8, the predictions are the same. The period for the *reference* motion is $T_r = 10.736096$, while the period for the *general* motion is $T_g = 10.736089$. We must then compare $\phi_n(T_r) = 6.282935283$ with $\phi_b(T_g) = 6.282935163$. There is a small difference in the angular advance of both motions: $\Delta\phi = \phi_b(T_g) - \phi_n(T_r) \approx -1.20 \times 10^{-7}$. This difference should be considered *small*, since we need approximately $n = 73,000$ full cycles to produce a total difference of $\pi/36$ (five degrees). The conclusion is that if we are only interested in the *total advance*, the *reference* equations produce the same results. However, the difference is important for times close to $T/4$, when the bob is at its closest approach to the vertical.

10 Accuracy of the classical hypotheses

The analytical solution given in Sect. 7 corresponds to a pendulum where not only energy dissipation is neglected and the parametric energy feed is off, but which also satisfies Eq. 37, the constancy of the vertical component of the angular momentum, and Eq. 34, the constancy not of the energy given by Eq. 26, but of the expression that neglects the term going as Ω^2, as written in Eq. 34. Clearly, the work reported in Sect. 9 is the right tool to investigate the accuracy of the classical hypotheses.

10.1 The *constancy* of the areal velocity

Having solutions $\theta_b(t)$ and $\phi_b(t)$ along a full cycle, we can calculate the areal velocity φ with the help of Eq. 35 and obtain a graphical idea of its *constancy*. This result, however, depends on the angular position of

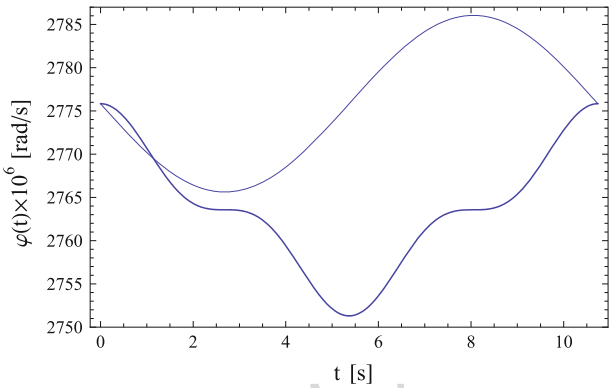

Fig. 9 The areal velocity along a full cycle for a Foucault pendulum starting at: $\phi_0 = 0$ (*thick line*), $\phi_0 = \pi/2$ (*thin line*)

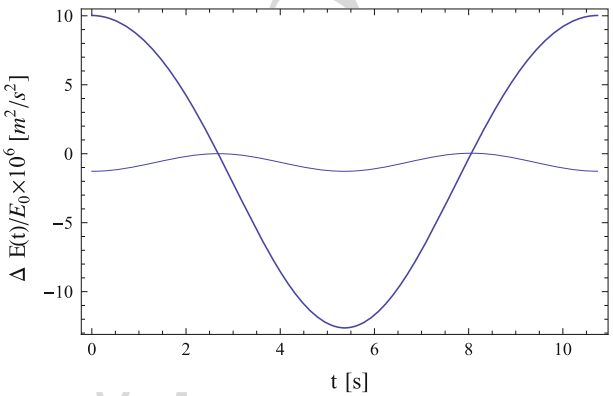

Fig. 10 The total energy $[(E(t) - E(T/4))/E_0] \times 10^6(t)$ along a full cycle for a Foucault pendulum starting at: $\phi_0 = 0$ (*thick line*), $\phi_0 = \pi/2$ (*thin line*)

the plane of oscillation of the pendulum, that is, on $\phi(0)$. If $\phi(0) = 0$, the *plane* of oscillation of the pendulum is along the north–south direction, while if $\phi(0) = \pi/2$, in the east–west direction. As Fig. 9 shows, it is only the shape that depends on $\phi(0)$, but the limits between which the areal velocity varies are essentially fixed, representing a variation of less than 0.75%. We can thus see that areal velocity is constant, the variation being less than 35 parts in one million in both extreme cases.

10.2 The *constancy* of energy

We next consider the energy E given by Eq. 34, whose constancy is used to establish the *reference* equations. A plot of $E(t)$ shows essentially a horizontal line. To see the small variation of this energy, we must plot the difference between $E(t)$ and some fixed value, say $E(T/4)$, its value when the bob is closest to the vertical. However, to get a real feeling of the difference $E(t) - E(T/4)$, we have plotted its ratio to the maximum kinetic energy E_0. Figure 10 is a plot of $(E(t) - E(T/4))/E_0$, as a function of time, from $t = 0$ to $t = T_q$. The thick (thin) line corresponds to a pendulum starting at $\phi_0 = 0$ ($\phi_0 = \pi/2$). The different behavior is due to the fact that a pendulum swinging in the north–south direction approaches and recedes more from the axis of rotation of the Earth than one swinging in the east–west direction. We can see that this fractional change is smaller than ten parts in a million!

11 The influence of dissipative forces

We now discuss the motion of the pendulum by dropping the hypothesis of no dissipative forces, while keeping the condition of no parametric energy feed.

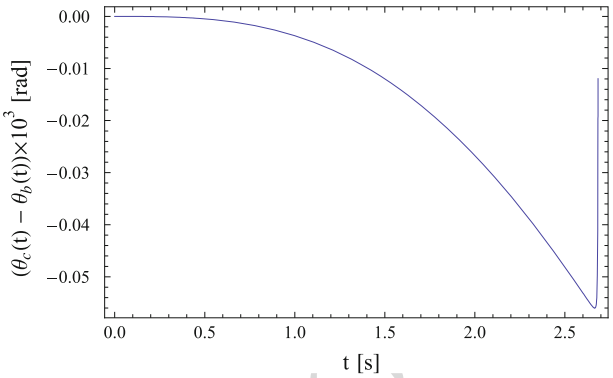

Fig. 11 Difference in angular excursion $\theta_c(t) - \theta_b(t)$ (i.e., difference between with and without dissipative forces) along the first quarter of a cycle

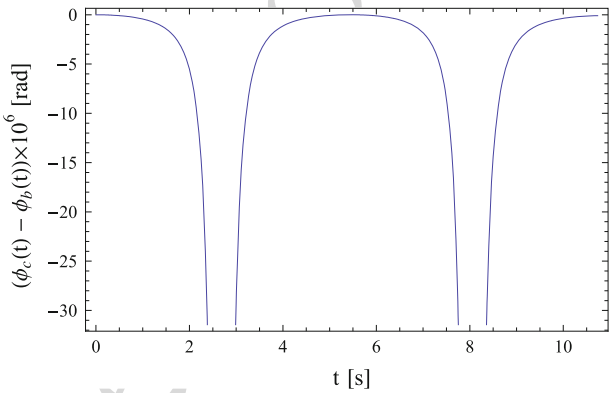

Fig. 12 Difference in azimuth advance along the first complete cycle. ϕ_c includes dissipative forces, whereas ϕ_b does not

Our differential equations (32)–(33), after setting $\dot{l} = 0$, involve only two unknowns: k_θ and k_ϕ, connected with the dissipative forces. The Rayleigh dissipation function, Eq. 29, shows that the rôle of k_ϕ is similar to that of k_θ. We shall suppose that

$$k_\phi = k_\theta = k = 0.000772. \tag{48}$$

Later, in this section, we shall indicate the method used to measure k. Let us call $\theta_c(t)$ and $\phi_c(t)$ the solutions to the Lagrange–Rayleigh equations. As expected, when $\theta_c(t)$ and $\theta_b(t)$, or $\phi_c(t)$ and $\phi_b(t)$ are plotted together, they give rise to only one graphic, that is, their difference is smaller than the thickness of the plot itself. We obtain more information by plotting the differences $\theta_c(t) - \theta_b(t)$ and $\phi_c(t) - \phi_b(t)$. The first one is shown in Fig. 11 along the first quarter of a cycle, while Fig. 12 shows the difference $\phi_c(t) - \phi_b(t)$ along a complete period.

In spite that there is a *large* difference (difficult to measure) when the bob approaches the vertical, the difference in azimuth advance for a whole period is $\Delta\phi \approx 1.11 \times 10^{-7}$. This difference may be considered *small* since it needs 783,595 whole periods to accomplish a total difference of $\pi/36$ (five degrees).

With the help of $\theta_c(t)$ and $\phi_c(t)$, we can plot the areal velocity φ given by Eq. 35. The thick (dashed) line of Fig. 13 shows the areal velocity for a pendulum without (with) dissipative forces.

Concerning the total energy E given by Eq. 34, the corresponding plots are shown in Fig. 14 where the thin line corresponds to the case free of dissipative forces. Its *apparently constant* value is due to the scale of the vertical axis.

The decrease in the angular excursion from the vertical as the pendulum accomplishes several whole cycles is a known fact. The method we used to pursue the solution across several cycles was based in the solution to one cycle: We obtained the numerical solution corresponding to the initial conditions of Eq. 42 and a time interval slightly larger than the real period. This time interval is $[0, (21/20)T_o]$, where $T_o = 2\pi\sqrt{l/g}$ is the period of a pendulum with very small amplitude. To determine the *period* of our pendulum, we found the

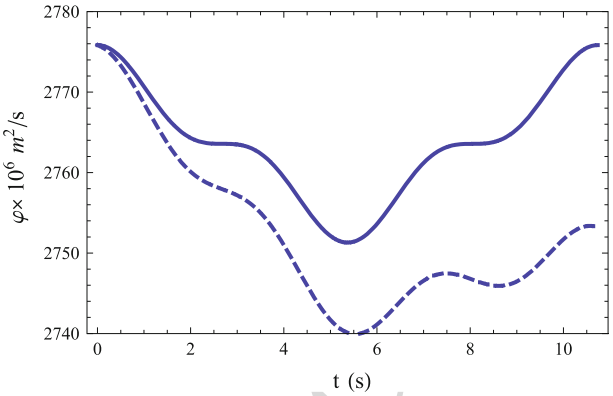

Fig. 13 The areal velocity φ along a complete cycle of a pendulum without (with) dissipative forces is shown by the solid (*dashed*) line

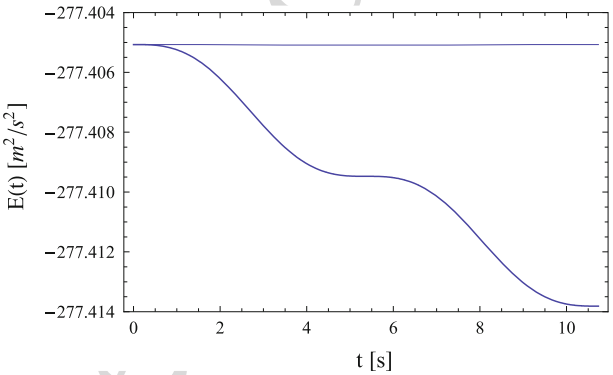

Fig. 14 The total energy of a pendulum, along a complete cycle, with (without) dissipative forces is shown by the thin (*thick*) line

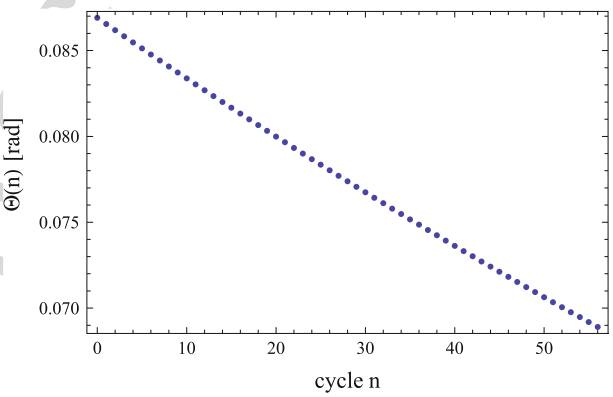

Fig. 15 The maximum angular excursion $\Theta(n)$ for the first 57 cycles

nearest root T_f from $t = (21/20)T_o$ to the equation

$$\dot{\theta}(t) = 0. \tag{49}$$

This condition identifies completely the end of the cycle. The numerical values of $\theta(T_f)$, $\phi(T_f)$, $\dot{\theta}(T_f) = 0$ and $\dot{\phi}(T_f)$ are then used as initial conditions to solve for the second cycle. Iterating this procedure, we determined the solution along the first 57 cycles, and from this solution, we extracted the information concerning the numerical decrease in the maximum angular excursion and the variation of the *period* as functions of the cycle number. These results are shown in Figs. 15 and 16.

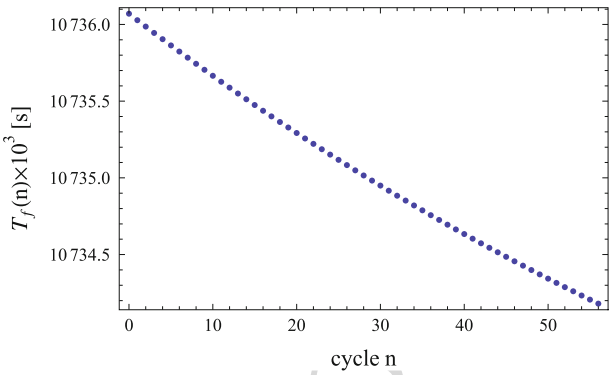

Fig. 16 The period T_f of the pendulum with dissipative forces for the first 57 cycles

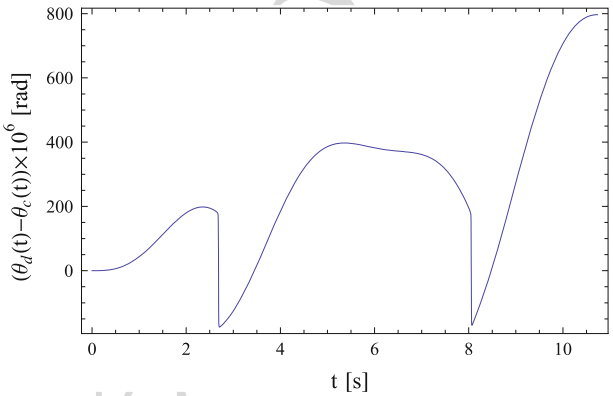

Fig. 17 $\theta_d(t)$ and $\theta_c(t)$ are solutions to the general equations. θ_d corresponds to the case with dissipative forces and parametric energy feed, whereas θ_c to the case with dissipative forces and without parametric energy feed

Working with our pendulum, we measured the maximum angular excursion Θ_e at the end of the 57th cycle and determined, since $\Theta(57)$ is a decreasing function of k, by trial and error, the value of k such that $\Theta_e = \Theta(57)$ within experimental accuracy.

12 Effect of dissipative forces and of parametric energy feed

The *parametric energy feed* is produced [4,5] by changing the length l of the pendulum by means of an external mechanism according to the law:

$$l(t) = l_o + \epsilon_o \sin 2\omega t \tag{50}$$

where $l_o = 28.5$ m is the length of our pendulum, $\omega = 2\pi/T_o$, the angular frequency of the pendulum, $\epsilon_0 = 0.08$m, the length of the *parametric perturbation*.[4] In this section, we report our results corresponding to one cycle whose initial conditions at $t = 0$ are given by Eq. 42.

Let us call $\theta_d(t)$ and $\phi_d(t)$ the numerical solutions to Eqs. 32 and 33. When these solutions are plotted side by side with $\theta_c(t)$ and $\phi_c(t)$, a very small difference may be discovered. The best information is obtained plotting the differences:

- $\theta_d(t) - \theta_c(t)$, plotted in Fig. 17, shows a net increase in amplitude by the end of the cycle. The two *apparently abrupt* changes, observed as the bob approaches the vertical, are *continuous* in the mathematical sense.

[4] The value of ϵ_0 may be continuously varied from 0 to 0.1 m.

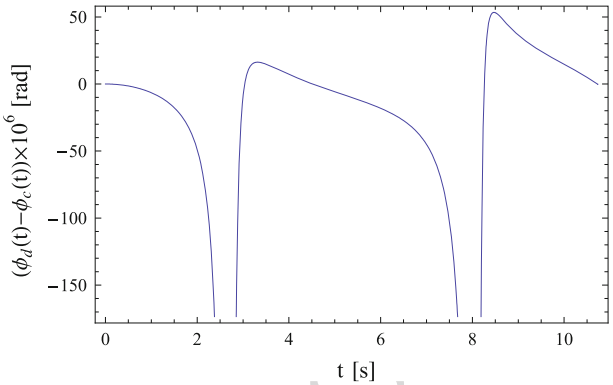

Fig. 18 ϕ_d and ϕ_c are solutions to the general equations, both taking dissipative forces into account. ϕ_d includes parametric energy feed whereas ϕ_c does not

- $\phi_d(t) - \phi_c(t)$ is shown in Fig. 18. Remark that for a whole cycle, there should be no difference in the azimuth advance, that is, $\phi_d(T) - \phi_c(T) = 0$ where T is the period of the pendulum. However, when the bob approaches the vertical, these difference may attain large values.

The numerical difference in azimuth advance is -1.69×10^{-7}. In fact, our results do not contend that the azimuth velocity is a constant, but that the mean azimuth velocity, under parametric energy feed and dissipative forces, computed along complete cycles, is equal, within $1.69 \times 10^{-7}/T_o \approx 2 \times 10^{-8}$, to the corresponding velocity for a text-book-Foucault-pendulum.

13 Time behavior of the forces connected with the energy feed

We can solve for $\ddot{\theta}$ and $\ddot{\phi}$ from Eqs. 32 and 33, the general equations of motion, in two different conditions: first, with parametric energy feed and second, without it, retaining dissipative forces in both cases. The resulting expressions give, except for a factor, the corresponding generalized forces. We are interested in the differences between with and without parametric energy feed, which have the same units as the angular acceleration. These differences, represented as f_θ and f_ϕ since they are connected with the generalized forces producing the energy feed, are given by:

$$\begin{aligned} f_\theta = I_m \{ & 4L\omega \left(\kappa\Omega \sin\phi - \dot{\theta}\right) \cos(2\omega t) \\ & + \left[\cos\theta \cos\phi \left(\kappa\rho\sigma\Omega^2 - g \sin\epsilon\right) + \sin\theta \left(\kappa^2\rho\Omega^2 - g\cos\epsilon\right)\right] \\ & \times \sin(2\omega t)\} \end{aligned} \tag{51}$$

$$\begin{aligned} f_\phi = I_m \{ & 4L\omega \left[\Omega(\sigma - \kappa \cot\theta \cos\phi) + \dot{\phi}\right] \cos(2\omega t) \\ & + \csc\theta \sin\phi \left(\kappa\rho\sigma\Omega^2 - g \sin\epsilon\right) \sin(2\omega t)\} \end{aligned} \tag{52}$$

where

$$I_m = \frac{\epsilon_0}{L(L + \epsilon_0 \sin(2\omega t))} \tag{53}$$

Since $\epsilon_0 \ll L$, I_m, and these forces are directly proportional to ϵ_0.

A plot of these forces is shown in Figs. 19 and 20. We have added three dots along the abscissae to identify three instants of time: $t = T/4$, $t = T/2$ and $t = 3T/4$. Remark that Fig. 19 is antisymmetric with respect to $t = T/2$. In the interval $[0, T/2]$, the generalized force is also antisymmetric with respect to time $t = T/4$. Starting at $t = 0$, the bob 'feels' initially a negative force, attaining a minimum at $t = 0.794$ s, when this force begins to increase, vanishing at $t = 1.514$, but increasing steadily up to $t = 2.64$, slightly less than $t = T/4$. The transition around $t = T/4$ is continuous, although the figure seems to show the contrary. This means that the motion in θ is accelerated negatively along $[0, 1.514]$, while positively along $[1.514, T/4]$. The *positive* area exceeds the *negative* area in 0.00008, producing thus a net increase in amplitude.

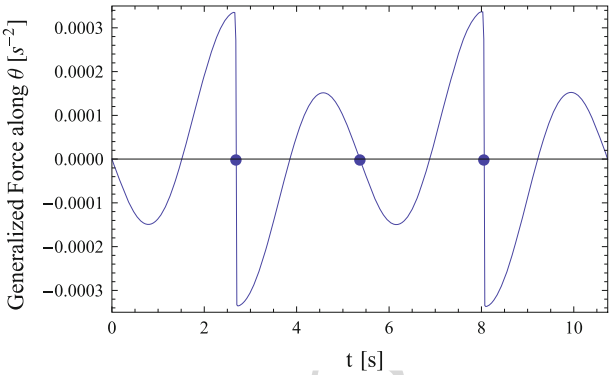

Fig. 19 Generalized force along θ, except for a factor, due to parametric energy feed

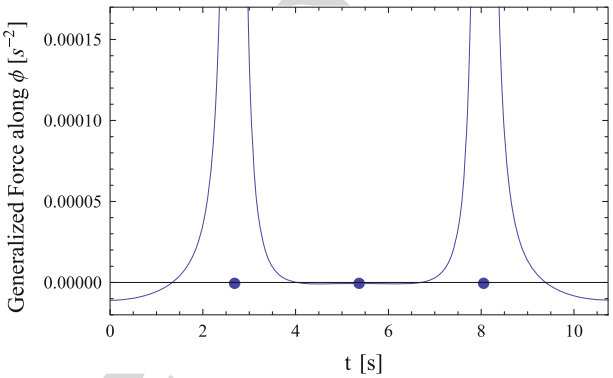

Fig. 20 Generalized force along ϕ, except for a factor, due to parametric energy feed

14 The complex cycle

Our pendulum was designed to be always in motion. From the practical point of view, according to our experience, the external mechanism responsible for the energy feed should be used as little as possible, to prevent wear in the cable or in the clutches, and to increase also the lifespan of the system. These conditions led us to choose a large value for ϵ_0, which after many trial-error experiments was finally set in $\epsilon_o = 0.08$ m. This choice, however, requires $n_1 = 57$ cycles without energy feed, followed by $n_2 = 25$ cycles with. We shall call *complex cycle* this combination of 82 whole cycles. The amplitude of our pendulum is 5^o, approximately constant when analyzed along a set of 82 cycles.

We then wrote a program that could determine the motion along the given 82 cycles, to determine the numerical value of k, Eq. 48, the constant connected to dissipative forces. The method used is: We proposed a numerical value for k, we solved the resulting differential equations for the complex cycle and compared the final with the initial amplitude. Since the final amplitude is a decreasing function of k, this was enough to determine the value of k that took the value indicated in Eq. 48. The difference between the initial and final value is

$$\theta_f - \theta_0 \approx 7.45 \times 10^{-7}. \tag{54}$$

There are three main results concerning the complex cycle. The first one, Fig. 21, concerns $\Theta(n)$, the maximum angular excursion of θ as a function of the number of the cycle.

The period of the pendulum $T(n)$, Fig. 22, as defined in the paragraph preceding Eq. 49, is a decreasing function of the number of cycle, while the pendulum is only submitted to the action of dissipative forces. As soon as the energy feed is applied, the period becomes an increasing function of this number. Figures 21 and 22 suggest that the period is a function of the angular excursion.

This fact suggested us to plot the period vs angular excursion. Figure 23 shows that there are two different periods for a given angular excursion, depending on whether there is or not energy feed, being slightly larger in the last case. The starting point is on the left-hand side, in the upper series of dots. The system goes down until

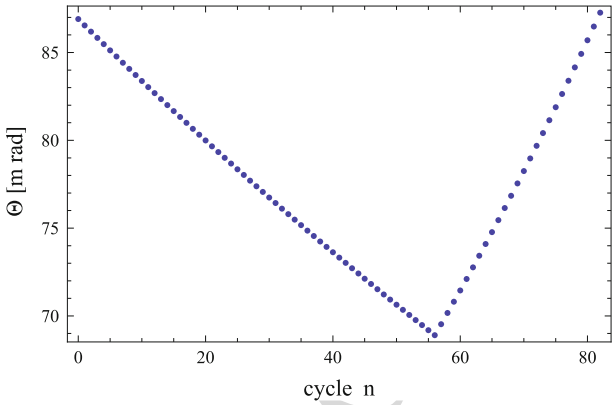

Fig. 21 Maximum angular excursion vs number of cycle. The first 57 cycles are without parametric energy feed, while the last 25, with

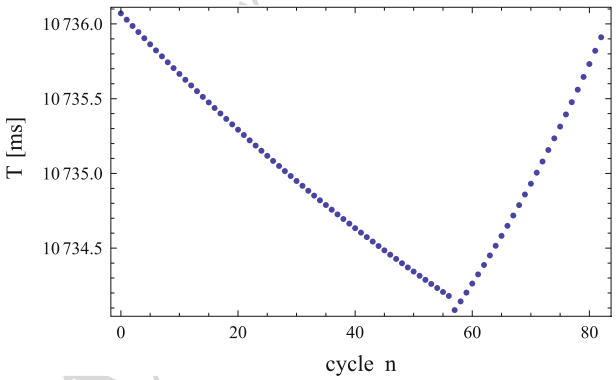

Fig. 22 The period of the pendulum as a function of cycle number. Notice that the total change is in the fifth and sixth figures only

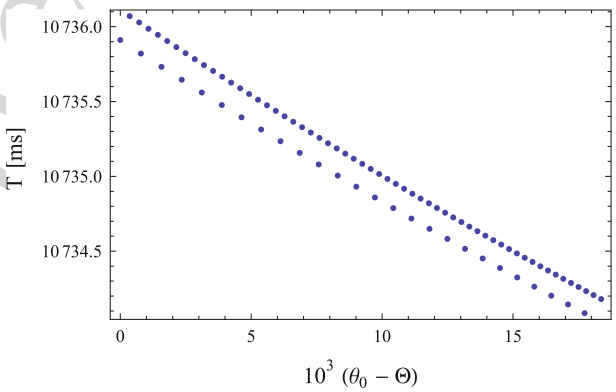

Fig. 23 The period T of the nth cycle of the pendulum as a function of $\theta_0 - \Theta(n)$, where $\Theta(n)$ is the maximum angular excursion from the vertical and $\theta_0 = \pi/36$. The initial state is at the *left upper* corner. The state goes down along the upper line of dots. The energy feed follows the lower line up to the initial state

the energy feed mechanism is applied, when the system goes up, along the lower line of dots, steadily, to return back to the initial condition. This means that the period is an increasing function of amplitude, possessing two branches, depending on whether the energy feed mechanism is on or not. Note that for a given amplitude, the difference is of the order of three parts in 10^6.

15 Conclusions

- The method of Runge–Kutta applied to the second-order reference equations produces the same time evolution as the analytical one within 3×10^{-19}.
- The method of Runge–Kutta may be applied to the Lagrange–Rayleigh equations for the Foucault pendulum subjected both to dissipative forces and parametric energy feed.
- The angular advance in the azimuth ϕ predicted by the reference equations and by the general equations is the same within 1.68×10^{-7} for a whole cycle.
- There are important differences between the motions predicted by the reference and general equations, with or without dissipative forces, with or without parametric energy feed, when the bob approaches the vertical.

References

1. Tobin, W.: The Life and Science of LÉON FOUCAULT. Cambridge University Press, Cambridge (2003)
2. Charron, M.: C. Rend. Acad. Sci. Paris. **192**, p. 208 26 janvier (1931)
3. Richard Crane, H.: Short Foucault pendulum: a way to eliminate the precession due to ellipticity. Am. J. Phys. **49**(11), 1004–1006 (1981)
4. Pippard, A.B.: The parametrically Maintained Foucault Pendulum and its perturbations. Proc. R. Soc. Lond. A **420**, 81–91 (1988)
5. de Icaza-Herrera, M., Castaño, V.M.: The Foucault pendulum revisited: normal vs anomalous behaviors (2008, submitted)
6. Landau, L.D., Lifshitz, E.M.: Mechanics **1**. §39. Pergamon Press (1960)
7. Landau, L.D., Lifshitz, E.M.: Mechanics **1**. §6. Pergamon Press (1960)
8. Goldstein, H.: Classical Mechanics, 2nd edn. Addison Wesley, Reading (1980)
9. Abramowitz, M., Stegun, I.A.: Hand Book of Mathematical Functions with Formulas, Graphs, and Mathematical Tables. National Bureau of Standards. Applied Mathematics Series (1964)